

**DEVELOPMENT OF THE MODIFIED ZEOLITE-A CATALYST FOR THE
DIRECT CONVERSION OF METHANE TO LIQUID HYDROCARBONS**

MOHAMMAD AFIFI FAIZ BIN AZHA @ AZAHAR

UNIVERSITI MALAYSIA PAHANG

UNIVERSITI MALAYSIA PAHANG

BORANG PENGESAHAN STATUS TESIS

JUDUL: DEVELOPMENT OF THE MODIFIED ZEOLITE-A CATALYST FOR THE DIRECT CONVERSION OF METHANE TO LIQUID HYDROCARBONS

SESI PENGAJIAN: 2007/2008

Saya **MOHAMMAD AFIFI FAIZ BIN AZHA @ AZAHAR**
(HURUF BESAR)

mengaku membenarkan kertas projek ini disimpan di Perpustakaan Universiti Malaysia Pahang dengan syarat-syarat kegunaan seperti berikut:

1. Hak milik kertas projek adalah di bawah nama penulis melainkan penulisan sebagai projek bersama dan dibiayai oleh UMP, hak miliknya adalah kepunyaan UMP.
2. Naskah salinan di dalam bentuk kertas atau mikro hanya boleh dibuat dengan kebenaran bertulis daripada penulis.
3. Perpustakaan Universiti Malaysia Pahang dibenarkan membuat salinan untuk tujuan pengajian mereka.
4. Kertas projek hanya boleh diterbitkan dengan kebenaran penulis. Bayaran royalti adalah mengikut kadar yang dipersetujui kelak.
5. *Saya membenarkan/tidak membenarkan Perpustakaan membuat salinan kertas projek ini sebagai bahan pertukaran di antara institusi pengajian tinggi.
6. **Sila tandakan (✓)

AKTA	<input type="checkbox"/>	SULIT	(Mengandungi maklumat yang berdarjah keselamatan atau kepentingan Malaysia seperti yang termaktub di dalam RAHSIA RASMI 1972)
	<input type="checkbox"/>	TERHAD	(Mengandungi maklumat TERHAD yang telah ditentukan oleh organisasi/badan di mana penyelidikan dijalankan)
	<input checked="" type="checkbox"/>	TIDAK TERHAD	

Disahkan oleh

(TANDATANGAN PENULIS)

Alamat tetap:
No. 1361-A, Lorong 4, Kampung Besut,
24000 Chukai, Kemaman
Tarikh: 30 April 2008

(TANDATANGAN PENYELIA)

Dr. Chin Sim Yee
Nama Penyelia

Tarikh: _____

- CATATAN:
- * Potong yang tidak berkenaan.
 - ** Jika tesis ini SULIT atau TERHAD, sila lampirkan surat daripada pihak berkuasa/organisasi berkenaan dengan menyatakan sekali sebab dan tempoh tesis ini perlu dikelaskan sebagai SULIT atau TERHAD.
 - ◆ Tesis dimaksudkan sebagai tesis bagi Ijazah Doktor Falsafah dan Sarjana secara penyelidikan, atau disertasi bagi pengajian secara kerja kursus dan penyelidikan, atau Laporan Projek Sarjana Muda (PSM).

“Saya/Kami* akui bahawa saya telah membaca karya ini dan pada pandangan saya/kami* karya ini adalah memadai dari segi skop dan kualiti untuk tujuan Penganugerahan Ijazah Sarjana Muda Kejuruteraan Kimia.”

Tandatangan :

Nama Penyelia I :

Tarikh :

Tandatangan :

Nama Penyelia II :

Tarikh :

Tandatangan :

Nama Penyelia III :

Tarikh :

**Potong yang tidak berkenaan*

**DEVELOPMENT OF THE MODIFIED ZEOLITE-A CATALYST FOR THE
DIRECT CONVERSION OF METHANE TO LIQUID HYDROCARBONS**

MOHAMMAD AFIFI FAIZ BIN AZHA @ AZAHAR

A thesis submitted in fulfillment of the
requirements for the award of the degree of
Bachelor of Chemical Engineering (Gas Technology)

**Faculty of Chemical and Natural Resources Engineering
Universiti Malaysia Pahang**

MAY 2008

I declared that this thesis entitled

‘Development of the modified Zeolite-A catalyst for the direct conversion of methane to liquid hydrocarbons’ is the result of my own research except as cited in the references. The thesis has not been accepted for any degree is not concurrently submitted candidature of any degree.

Signature :

Name of Candidates : MOHAMMAD AFIFI FAIZ BIN AZHA@AZAHAR

Date : 9 MAY 2008

Special dedicated to my beloved mother and father

ACKNOWLEDGEMENT

In the name of Allah the Most Gracious and Most Merciful

Alhamdulillah thank to Allah for giving me a strength and good health condition at last I be able to accomplish my undergraduate research report as scheduled. In this opportunity I would like express my appreciation to all people who involve directly or not directly in helping me to complete this thesis. There are many people who involve in and pay contribution for this thesis. The people who gave me guidance and share their times and experiences to give me full understanding and moral support to complete my thesis. I would like to express my special thanks to Dr. Chin Sim Yee and Mr. Syamsul Bahari Bin Abdullah for their will to share his experience, encouragement, guidance, critics and assistance to help me fulfil my thesis as a supervisor.

In this opportunity, I would like to thank all lecturers and staffs in Faculty of Chemical And Natural Resource Engineering University Malaysia Pahang especially teaching engineers who spend their time to give a space for completing this research. Indeed, I indebted all staffs and lectures for their endless support and encouragements.

Finally my endless thanks goes to my family and my fellow friends especially my classmates from 4BKG for their support and suggestions. May Allah bless us.
Wassalam

ABSTRACT

The characteristic of Zeolite-A loaded with iron and zinc on the direct conversion of methane to liquid hydrocarbons is investigated. Zeolite-A is loaded with different mass ratio of zinc and iron. Thermo Gravimetric Analysis (TGA), X-Ray Diffraction (XRD), and Fourier transform spectroscopy (FTIR) are used to analyze the physicochemical properties of the modified zeolite such as functional group, surface area and average diameter of unit cell. The absence of the iron content in the catalyst does not affect the framework and the crystalline of the catalyst but only affect the size of the unit cell and the surface area of the catalyst. As compare to zinc, it has modified the crystalline and framework of the catalyst. The result indicated that Zeolite-A with 8% of zinc and 2% of iron of metal doped is the most suitable catalyst for the methane conversion to liquid hydrocarbons. The catalyst has high thermal stability, high surface area, and high average diameter of unit cell and has low weight loss.

ABSTRAK

Kajian ciri-ciri Zeolite-A dengan campuran logam besi dan zink terhadap proses penukaran metana secara terus kepada hidrokarbon cecair telah dijalankan. Zeolite-A akan dicampur dengan nisbah jisim zink dan iron yang berbeza-beza. Thermo Gravimetric Analysis (TGA), X-Ray Diffraction (XRD), dan Fourier transform spectroscopy (FTIR) akan digunakan untuk mengesan fizikal kimia pemangkin yang telah diubahsuai seperti kumpulan berfungsi, luas permukaan dan diameter purata unit cell. Kehadiran unsur besi dalam pemangkin tidak mengubah rangka dan stuktur kristal tetapi hanya mengubah saiz unit sel dan luas permukaan pemangkin tersebut. Berbanding dengan unsur zink, ia mengubah rangka dan struktur kristal pemangkin tersebut. Keputusan menunjukkan bahawa Zeolite-A dengan campuran 8% zink dan 2% besi merupakan pemangkin yang paling sesuai untuk proses penukaran metana secara terus kepada hidrokarbon cecair. Pemangkin ini mempunyai kestabilan termal yang tinggi, permukaan pemangkin yang luas, saiz unit sel yang besar dan mempunyai kadar pengurangan jisim yang rendah.

TABLE OF CONTENT

CHAPTER	TITLE	PAGE
	TITLE PAGE	i
	DECLARATION OF ORIGINALITY	ii
	EXCLUSIVENESS DEDICATION	iii
	ACKNOWLEDGEMENT	iv
	ABSTRACT	v
	ABSTRAK	vi
	TABLE OF CONTENT	vii
	LIST OF TABLES	x
	LIST OF FIGURES	xi
	LIST OF SYMBOL	xii
	LIST OF APPENDICES	xiii
1	INTRODUCTION	1
	1.1 Research Background	1
	1.2 Problem Statement	3
	1.3 Research Objective	4
	1.4 Scope of Research	4
2	LITERATURE REVIEW	5
	2.1 Methane Convert to Higher Hydrocarbon	5
	2.2 Zeolite	6
	2.3 Zeolite Acidity	8

2.4	Ga-HZSM-5	9
2.5	W-HZSM-5	10
2.6	Zn-ZSM-5	10
2.7	Mo-ZSM-5	11
2.8	Mo-HZSM-5	13
2.9	Characterization of Catalyst Using X-Ray Diffraction	14
2.10	Characterization of Catalyst Using TPD	15
2.11	Characterization of Catalyst Using TGA	16
2.12	Characterization of Catalyst Using FTIR	16
3	METHODOLOGY	18
3.1	List of Materials	18
3.2	Overall Methodology	19
3.2.1	Zeolite A	19
3.2.2	Synthesis of Fe/Zn-Zeolite-A	19
3.2.3	Catalyst Characterization	20
3.2.3.1	X-Ray Diffraction (XRD)	20
3.2.3.2	Fourier Transform Infrared Spectroscopy (FTIR)	20
3.2.3.3	Thermo Gravimetric Analysis (TGA)	21
4	RESULTS & DISCUSSION	22
4.1	XRD Characterization	22
4.2	FTIR Characterization	26
4.3	TGA Characterization	29
4.4	General Discussion	33
5	CONCLUSION & RECOMMENDATION	36
5.1	Conclusion	36
5.2	Recommendation	37

REFERENCES

APPENDIX A

LIST OF TABLES

NO.	TITLE	PAGE
1.1	The typical composition of natural gas before is refined (Kvenvolden, 1995)	1
2.1	The Si/Al ratio and unit cell parameters of zeolites (Amin <i>et al.</i> , 2001)	15
2.2	Nitrogen adsorption data (Amin <i>et al.</i> , 2001)	16
2.3	Infrared band positions of ZSM-5 and metal loaded ZSM-5 (Nor Aishah <i>et al.</i> , 2003)	17
3.1	List of materials	18
3.2	Mass of zinc, iron and zeolite for each sample	20
4.1	Crystallinity, average diameter of unit cell and rank average diameter of unit cell	22
4.2	Intensity of the highest peak in x-ray diffractogram	26
4.3	Crystallinity, average diameter of unit cell and Intensity of the highest peak in x-ray diffractogram	33
4.4	Peak at $900 - 910 \text{ cm}^{-1}$ and changing of the samples in FTIR characterization	33
4.5	Result of TGA characterization	34

LIST OF FIGURES

NO.	TITLE	PAGE
2.1	The Structure of Zeolite (Ch. Baerlocher <i>et al.</i> , 2001)	7
2.2	Acid Site (Subhash Bhatia <i>et al.</i> , 1990)	9
2.3	Formation of benzene and naphthalene from methane on Mo/ZSM-5 (Jean-Philippe Tessonier <i>et al.</i> , 2007)	11
2.4	Different model of Mo anchoring on Brønsted acid sites of the ZSM-5 (R.W. Borry <i>et al.</i> , 1999)	13
2.5	XRD diffractogram of HZSM-5 and Ga-HZSM-5 zeolite catalyst (Amin <i>et al.</i> , 2001)	14
2.6	Infrared spectra (Amin <i>et al.</i> , 2003)	17
3.1	Experimental Work Flow	19
4.1	X-ray diffractogram of sample 1	23
4.2	X-ray diffractogram of sample 2	23
4.3	X-ray diffractogram of sample 3	24
4.4	X-ray diffractogram of sample 4	24
4.5	X-ray diffractogram of sample 5	25
4.6	Wavenumber vs absorbance using FTIR	28
4.7	Weight Loss (%) vs Temperature for sample 1	29
4.8	Weight Loss (%) vs Temperature for sample 2	29
4.9	Weight Loss (%) vs Temperature for sample 3	30
4.10	Weight Loss (%) vs Temperature for sample 4	30
4.11	Weight Loss (%) vs Temperature for sample 5	31

LIST OF SYMBOLS

TGA	Thermo Gravimetric Analysis
FTIR	Fourier Transform Infrared Spectroscopy
XRD	X-Ray Diffraction

LIST OF APPENDICES

APPENDIX	TITLE	PAGE
A	Result XRD Sample 1	42
	Result XRD Sample 2	43
	Result XRD Sample 3	44
	Result XRD Sample 4	45
	Result XRD Sample 5	45

CHAPTER 1

INTRODUCTION

1.1 Research Background

Natural gas consists of mixture of hydrocarbon gases. The characteristic of the natural gas is colorless, shapeless, and odorless in its pure form. Natural gas is formed primarily of methane but it also includes ethane, propane, butane and pentane. Table 1.1 show outlines the typical makeup of natural gas before it is refined. Natural gas is considered 'dry' when it is almost pure methane, having had most of the other commonly associated hydrocarbons removed. When other hydrocarbons present, the natural gas is 'wet' (Thomas and Dawe, 2003).

Table 1.1 The typical composition of natural gas before it is refined
(Kvenvolden, 1995)

Typical Composition of Natural gas		
Methane	CH ₄	70-90%
Ethane	C ₂ H ₆	0-20%
Propane	C ₃ H ₈	0-20%
Butane	C ₄ H ₁₀	0-20%
Carbon Dioxide	CO ₂	0-8%
Oxygen	O ₂	0-0.2%
Nitrogen	N ₂	0-5%
Hydrogen Sulphide	H ₂ S	0-5%
Rare Gases	A, He, Ne, Xe	trace

In the last several decades, methane represents over 90% of the natural gas content and hence it is considered as promising source with high hydrocarbon content (Mat *et. al.*, 1999). However, not all the available and produced methane is utilized. A lot of effort has been considered toward the conversion of methane to value-added products such as transportable liquid hydrocarbons and chemicals. Traditionally, there are two competing demands for natural gas. It is used as a clean fuel in power generation, industrial kilns and furnaces, vehicles, and domestic heating. Natural gas is also demanded as a feedstock for petrochemical and chemical industries (Mat *et. al.*, 1999).

Gas to liquids or GTL is a refinery process to convert natural gas or other gaseous hydrocarbons into longer-chain hydrocarbons (Aguiar *et. al.*, 2005). Methane-rich gases are converted into liquid fuels either via direct conversion or via syngas as an intermediate, using the Fischer Tropsch process (Yagi *et. al.*, 2005). Using such processes, refineries can convert some of their gaseous waste products into valuable fuel oils, which can be sold as or blended only with Diesel fuel (Vosloo, 2001). The process may also be used for the economic extraction of gas deposits in locations where it is not economic to build a pipeline. This process will be increasingly significant as crude oil resources are depleted, while natural gas supplies are projected to last into the 22nd century (Wittcoff *et. al.*, 2004).

The direct conversion of natural gas to liquid hydrocarbons has not yet been successfully economized in an inexpensive process. The conversions of methane to gasoline by direct routes are still at low activity and selectivity (Amin *et al.*, 2006). These processes are possible if the reaction is carried out by controlled oxidation over a suitable catalyst (Mat *et. al.*, 1999). Recent studies have shown that modification of ZSM-5 zeolite by ion exchange, direct synthesis or wet impregnation method with metal oxides of different size and chemical properties are very important to control its acidity and shape selectivity. These modification methods led to an improvement in the catalytic activity and gasoline selectivity. When the acidity is increased by exchanging the zeolite with alkali metal cations, the conversion of methane to hydrocarbons is slightly enhanced. As a result, the metal containing

ZSM-5 can produce higher conversion hydrocarbons in methane oxidation (Amin *et. al.*, 2004).

The performance for direct methane conversion to higher hydrocarbons mainly depends on the physicochemical properties of the catalyst and this process uses zeolite as a catalyst. Physicochemical properties such as surface area and thermal stability are the factors to achieve the higher conversion and quality for this process. Modification by incorporation of elements of different size and different chemical features on zeolite is important to control the acidity and the shape selectivity of a specific zeolite structure.

1.2 Problem Statement

Numerous recent researches have demonstrated the feasibility of direct transformation of methane into products of higher added values such as olefins, aromatics and oxygenous derivatives. These processes are possible if the reaction is carried out by controlled oxidation over a suitable catalyst.

In practice, two routes for direct methane conversions to higher hydrocarbons have been identified. There are oxidative coupling and methane aromatization. A lot of efforts have led to a significant increase in the activity and selectivity of the applied catalyst. Unfortunately, the maximum yield obtained is about 20%, which means that the process is economically unfeasible (Huggil *et. al.*, 2005). In the partial oxidation process, methane reacts with oxygen in the presence of catalyst to produce methanol. Unfortunately, the yield of methanol is too low (below 10%) and beyond industrial interest (Zhang *et. al.*, 2002; Michalkiewicz, 2004, Michalkiewicz, 2006). Direct conversion of methane to mainly ethane and ethene has been observed over fluorinated H-mordenite zeolite at 525°C, but with very poor methane conversion far below 1% (Kowalak *et. al.*, 1988). These low conversions are quite expected due to an unfavorable thermodynamic equilibrium at temperatures below 1000°C.

The application of zeolite for plasma catalytic methane conversion (PCMC) to higher hydrocarbons at very low gas temperature (room temperature to 200oC) by using Zeolites NaY, HY, NaX, NaA, Linde Type 5A and Na-ZSM-5 have been tested (Chang-jun Liu, 1999). NaA showed produce higher methane conversion (49%) compare using Na-ZSM-5 (44.6%) (Chang-jun Liu, 1999).

The present study focuses on the direct conversion of methane to liquid hydrocarbons. In order to overcome the current problems, the Zeolite-A will be doped with iron and zinc with different mass ratio in order to change the structure catalyst, thermal stability and other physicochemical to improve the quality of catalyst.

1.3 Research Objective

The objectives of this research are to:

1. To synthesis the Fe/Zn-Zeolite-A catalyst.
2. To study the physicochemical properties of the modified catalyst.
3. To relate the physicochemical properties of the catalyst with the conversion of methane to the liquid hydrocarbons.

1.4 Scope of Research

The scopes of this study are divided into four stages:

- Preparation and modification of catalysts
- Characterization of the catalyst for its physicochemical properties
- Compare the physicochemical properties of modified zeolite with unmodified zeolite and previous research.
 - Predict the catalyst performance of methane conversion to liquid hydrocarbons based on the physicochemical properties of the catalyst.

CHAPTER 2

LITERATURE REVIEW

2.1 Methane Convert to Higher Hydrocarbon

The first step to convert methane to higher hydrocarbons is methane oxidation that will produce olefin. Higher hydrocarbons will be produced from reaction of olefin through oligomerization, dehydrocyclization and aromatization using zeolite base catalyst according to the reaction scheme below:



The combination of the oxidative catalysis of methane with acid catalyst in a single catalytic process over bifunctional oxidative acid catalyst would be possible to convert methane directly to liquid hydrocarbon. This could be done by modifying pentasil zeolite catalyst with a suitable element. One possibility of modifying zeolites is the replacement of some of the silicon and aluminum with transition metal (Mat *et al.*, 2006).

Numerous catalysts have been discovered which possess different activities and selectivities for methane conversion to higher hydrocarbon. Most of them are based on metal or transition metal oxides, which are often supported on silica and alumina.

Direct partial oxidation of methane with O₂ to higher liquid hydrocarbons over transition metal containing ZSM-5 catalyst is reported (Han *et al.*, 1994; Amin *et al.*, 2004). Han *et al.* (1994) found that the successful methane conversion to hydrocarbons can be done over metal-containing ZSM-5 catalyst to two effects:

- i. Ability of the metal to show some limited activity to generate olefins from methane.
- ii. Sufficient low olefin oxidation activity to allow the olefin produced to remain in the system.

Han *et al.* (1994), found that when Zn loaded into ZSM-5 beyond one wt% metal, it potentially to reduce desired catalyst acidity needed for the conversion of methanol produced to C₅₊. During the early days, another synthetic zeolite (HZSM-5 Zeolite) was found to be a suitable catalyst for the conversion of the methane to higher hydrocarbons. The acidic HZSM-5 zeolite catalyst has shown a reasonable good oligomerization performance for olefin products to higher hydrocarbons.

2.2 Zeolites

By the conventional definition, zeolites are microporous aluminosilicates. This definition has been modified within the past years and nowadays isomorphously substituted materials, like for example gallosilicates, titanosilicates or aluminophosphates, are also called zeolites or zeolitic materials. Microporosity (pores with diameters below 2 nm) is an intrinsic feature of all these materials and is caused by channels and cavities within the crystal structures of zeolites (Baerlocher *et al.*, 2001).

The structure of zeolite as shown (Figure 2.1) consists the primary building units which cations coordinated tetrahedrally by oxygen. These tetrahedral are connected via corners, thus forming the crystal structure of the specific zeolite.

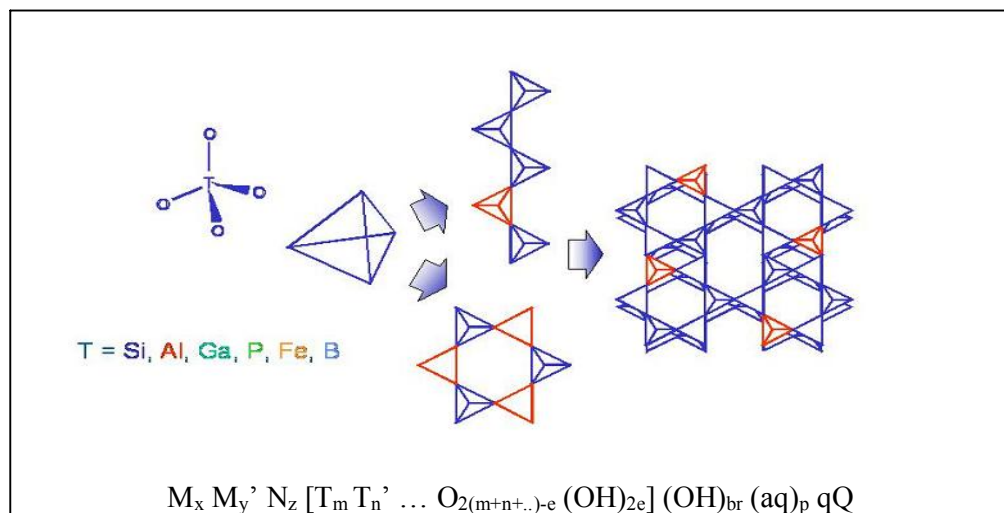


Figure 2.1 The Structure of Zeolite (Baerlocher *et al.*, 2001)

About 140 different zeolite structures are known of which about 40 are found in natural zeolites. The nomenclature of zeolites is rather confusing since every company is using its own names and abbreviations (Akporiaye *et al.*, 2001). To overcome this problem, a three-letter code system has been developed. These codes are assigned to specific structure type name *Linde Type A* (Meier *et al.*, 1987). This structure type is found in various materials, as for example in aluminosilicates, aluminogermanates, gallophosphates or silicoaluminophosphates. A collection of all known zeolite structures can be found in the atlas of zeolite framework types or on the web page of the international zeolite association (Ch. Baerlocher *et al.*, 2001).

Zeolite-A exhibits the LTA (Linde Type A) structure and has a 3-dimensional pore structure with pores running perpendicular to each other in the x, y, and z planes, and is made of secondary building units 4, 6, 8, and 4-4. The pore diameter is defined by an eight member oxygen ring and is small at 4.2Å. This leads into a larger cavity of minimum free diameter 11.4Å. The cavity is surrounded by eight sodalite cages (truncated octahedra) connected by their square faces in a cubic structure.

The unit cell is cubic ($a = 24.61\text{Å}$) with Fm-3c symmetry. Zeolite-A has a void volume fraction of 0.47, with a Si/Al ratio of 1.0. It thermally decomposes at 700°C. (Subhash Bhatia, 1990). Zeolite-A is of much interest because its supercage

structure is useful in spacio-specific catalysis. The inner cavity is large enough for structure changing reactions to take place, but the small pore means only a specific structure can get into the cavity for reaction, typically n-paraffins and olefins. One use is in paraffin cracking. The small entry pore is selective towards linear paraffins, and cracking can occur on sites within the supercage (alpha-cage) to produce smaller chain alkanes. Zeolite-A is also widely used in ion exchange separation (Ribeiro *et al.*, 1984)

2.3 Zeolite Acidity

The concept that solid surfaces may be acidic arose from the observation that hydrocarbon reactions such as cracking that are catalyzed by acid treated clays or silica alumina, give rise to a much different product distribution than those obtained by thermal reaction (Knozinger *et al.*, 1997). These solid catalyzed reactions exhibit features similar to reaction catalyzed by mineral acids. By analogy to solution chemistry, it is postulated that the primary requirement for catalyst activity is that the solid be acidic and be capable of forming carbonium ions by reaction with a hydrocarbon (Subhash Bhatia *et al.*, 1990).

An acid site may be of the Bronsted type in which it denotes a proton to an unsaturated hydrocarbon, or of the Lewis type in which it acts as an electron acceptor, removing a hydride ion from a hydrocarbon (Pfeifer *et al.*, 1997). Acid catalysis is important in catalytic reforming, cracking, hydrocracking, isomerization, hydrodewaxing, alkylation and dealkylation (Farcasiu *et al.*, 1998). It is therefore important to be able to measure acidity and to rank solids as possible candidates for improvement of the yields of the processes.

The general definition of an acid is an electron-pair acceptor. The Bronsted acid site is able to transfer a proton from the solid to the absorbed molecule while the Lewis acid site is able to accept an electron pair from the adsorbed molecule and a coordinative bond with the surface is formed is shown in Figure 2.2.

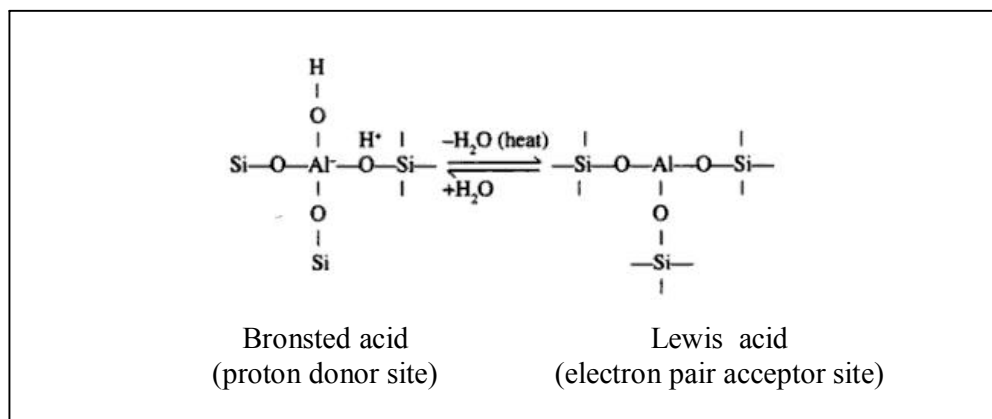


Figure 2.2 Acid Site (Subhash Bhatia *et al.*, 1990)

A description of acidity in general and surface acidity more specifically, requires the determination of the nature, the strength, and the number of acid sites. A solid acid is capable of transforming an adsorbed basic molecule into its conjugated acid form (Artioli *et al.*, 2001).

The catalyst acidity indicated the total amount of acid sites of modified zeolite is higher than ZSM-5. The metal-loaded will increase the acidity of the catalyst and improve the conversion of the process (Amin *et al.*, 2006).

2.4 Ga-HZSM-5

Gallium is one of the potential elements that could modify the properties of zeolites. Over this catalyst, higher quality gasoline yield was obtained in the oxidative methane conversion (Anggoro, D. D. *et al.*, 1998). Ga loaded on HZSM-5 is claimed to be very efficient for the aromatization of light alkenes and alkanes (Vermeiren *et al.*, 1989), and has the potential to convert methane to liquid hydrocarbons with high selectivity (Anggoro, D. D. *et al.*, 1998). HZSM-5 was modified with gallium by ion exchange to create a bifunctional catalyst with sites active in both acid catalysed and oxidation reactions for the conversion of methane to liquid hydrocarbons in a single catalytic step. The prepared catalyst, Ga-HZSM-5,

could act as a better bifunctional catalyst than its parent catalyst, HZSM-5 zeolite (Mat *et al.*, 1999).

2.5 W-HZSM-5

The W-HZSM-5 based catalyst was found to be a highly active catalyst for methane dehydroaromatization in the absence of oxygen (Zeng *et al.*, 2001). The catalyst showed a high activity and a high heat resistivity under reaction temperature of 1073 K. It was also reported that the addition of a second metal component into the catalyst by sequence impregnation method such as Zn (or Mn, La, Mg, Li) on W/HZSM-5 (Xiong *et al.*, 2001) enhanced the catalytic performance. The work reported by Xiong *et al.*, (2001) demonstrated that the catalyst with medium strength acidity could improve the dehydroaromatization of methane.

2.6 Zn-ZSM-5

In FT-IR study showed that zinc in the cationic position causes the generation of Lewis acid sites and decrease of the Bronsted. Disproportionation of toluene continuously decreases with increasing amount of Zn indicating the decline of the number of Bronsted acid site by introduction of zinc into zeolites. Aromatization of n-hexane on acid ZSM-5 zeolite is affected by the particle properties of the zeolite. The activity/selectivity of monofunctional acid catalysts is significantly higher on the HZSM-5 sample that has particles of smaller size, probably mainly due to the higher external surface of the zeolite (Agáta Smiešková *et al.*, 2004).

The selectivity of Zn-ZSM-5 catalysts continuously rises with increasing amount of Zn in the zeolite. This indicates the increase of the concentration of olefins precursors of aromatics in the reaction mixture due to the dehydrogenation activity of Zn species. Results showed that at higher Zn concentration the performance of Zn-

ZSM-5 catalysts is very different probably due to the fact that Zn species in the ZSM-5 zeolites in the case of higher Zn concentration are of different types (Agáta Smiešková *et al.*, 2004). The distances between the adjacent Al atoms in the zeolite framework affect the position of the zinc cations and determine if isolated or oxygen-bridged cationic species of Zn are created in the catalyst (A. Hagen *et al.*, 1994).

From the technological point of view it is important that the results call attention to the fact that besides of the composition and the acidity of the Zn-ZSM-5 catalysts, also the particle properties and aluminum distribution in the framework of the zeolite can affect the effectivity of Zn-ZSM-5 catalysts in aromatization of light alkanes (Agáta Smiešková *et al.*, 2004).

2.7 Mo-ZSM-5

Many progresses have been achieved since the first report on methane dehydro-aromatization over Mo/ZSM-5 in 1993 (L.Wang *et al.*, 1993). It is now generally accepted that the reaction takes place in two steps (Y.H. Kim *et al.*, 2000). In the early stages of the reaction, the molybdenum oxide is converted to MoC_x that later performs the CH₄ dehydrogenation and coupling to ethylene. Then, in a second step, the ethylene is oligomerized to benzene on the Brønsted acid sites of the zeolite (Figure 2.3). The location of the molybdenum plays a major role in this general scheme.

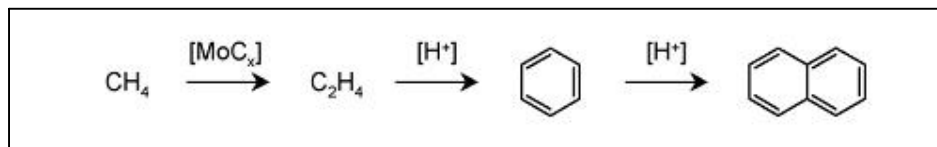


Figure 2.3 Formation of benzene and naphthalene from methane on Mo/ZSM-5 (Jean-Philippe Tessonier *et al.*, 2007)

Molybdenum oxide supported on classical supports like SiO₂, Al₂O₃ or TiO₂ is quickly carburized to MoC₂ under the reaction conditions and then only catalyses

the coke formation (F. Solymosi *et al.*, 1995). Different groups have also supported molybdenum oxide on various zeolites and mesoporous materials (Y. Shu *et al.*, 2001). Best results were obtained with zeolites ZSM-5 and MCM-22, presenting a two-dimensional porous network, with channels having a diameter of 5–6 Å that corresponds exactly to the kinetic diameter of the benzene molecule.

Tan *et al.* investigated in details the synthesis of 2 wt. % Mo/ZSM-5 and the consequences on its catalytic activity (P.L. Tan *et al.*, 2002). They found out that both common precursors, ammonium heptamolybdate (AHM) and MoO₃, are too large to penetrate the ZSM-5 channels during the impregnation process or during calcinations at temperatures below 600°C, in good agreement with previous work of Agudo *et al.* (A.L. Agudo *et al.*, 1992). However, at 700°C the MoO₃ vapor pressure becomes high enough (56 Pa) to allow MoO_x species start to diffuse inside the channels of the ZSM-5 (O. Knacke *et al.*, 1991).

Borry *et al.* further studied the diffusion of these species and their interaction with the Brønsted acid sites of the zeolite (R.W. Borry *et al.*, 1999). They provided clear evidence that Mo_xO_x vapor reacts with the acid sites to form a (Mo₂O₅)²⁺ cluster bridging two Brønsted sites of the zeolite (Figure 2.4a). Until now, this model was generally accepted. However, several groups provided contradictory elements. Mosqueira and Fuentes (2002) studied the spreading of molybdenum oxides on different supports, including ZSM-5 (L. Mosqueira *et al.*, 2002). They found by using diffuse reflectance UV spectroscopy that the molybdenum anchored on the support and exist in two different configurations: Mo₂O₇ dimer as predicted by Borry *et al.*, but also as tetrahedral MoO₄ monomer. Mosqueira and Fuentes do not make further hypothesis about the anchoring of this monomer. MoO₂²⁺ clusters could bridge two Brønsted acid sites, like for H–Y zeolites (Figure 2.4b) (H. Minming *et al.*, 1987). DFT calculations performed by Zhou *et al.* demonstrated that grafting could also occur via a MoO²⁺ cluster bridging two neighboring oxygen atoms (Figure 2.4c) (D. Zhou *et al.*, 2001).

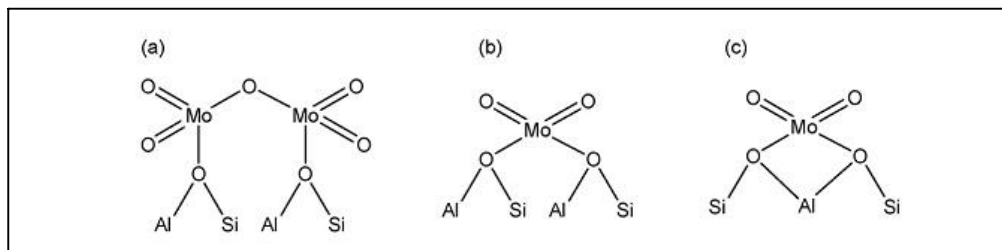


Figure 2.4 Different model of Mo anchoring on Brønsted acid sites of the ZSM-5 (R.W. Borry *et al.*, 1999)

2.8 Mo-HZSM-5

Recently, it has been shown that supported molybdenum, preferentially Mo supported on H-ZSM-5, is active and selective for benzene aromatic from methane (Y. Xu *et al.*, 1995). It was clearly established that at high temperature under CH_4 molybdenum in Mo-HZSM-5 was reduced and formed Mo_2C species (D. Wang *et al.*, 1997) and further during the activation process of Mo-HZSM-5 molybdenum species migrated towards exchangeable sites in the zeolite framework (D. Wang *et al.*, 1997). It is generally reported that the activation of methane occurs on molybdenum active species forming ethylene as primary product C_2H_4 being converted into benzene over H^+ acid sites of the zeolite (Y. Xu *et al.*, 1995).

In a very recent work it was shown by contrast that acetylene was the primary product of the reaction of methane over Mo-HZSM-5 (P. Meriaudeau *et al.*, 1999), and the authors concluded that a possible route for the formation of benzene is the production of C_2H_2 on Mo sites. The aim of this work was to provide an integrated understanding on the nature of active sites operating during the aromatization of methane over Mo-H-ZSM-5 catalyst. The role of the zeolite was examined by comparing H-ZSM-5 and H-MCM-22 having different topology. The role of protons in the zeolite, in which protons apparently improved the catalytic performances, was examined, and a reaction mechanism was proposed.

2.9 Characterization of Catalyst Using X-Ray Diffraction

X-ray diffraction provides information on the structure and unit cell parameter of zeolites, XRD analyses of gallium loaded zeolites was typical of crystalline HZSM-5 and did not reveal clear XRD lines attributable neither to oxide phases nor to metal oxide clusters (Figure 2.5) and The unit cell parameters and unit cell volume of the zeolite catalysts are presented in Table 2.1. The unit cell volume of Ga-HZSM-5 is smaller than that of HZSM-5, due to the removal of some of the aluminium from the zeolite framework (Amin *et al.*, 2001). It because of the ionic radii of tetrahedral structure of Si^{4+} is lower than Al^{3+} , 0.40\AA and 0.53\AA , respectively (Szostak, *et al.*, 1989). So, as the aluminium framework decrease, the unit cell parameters decrease, and the unit cell volume also decrease.

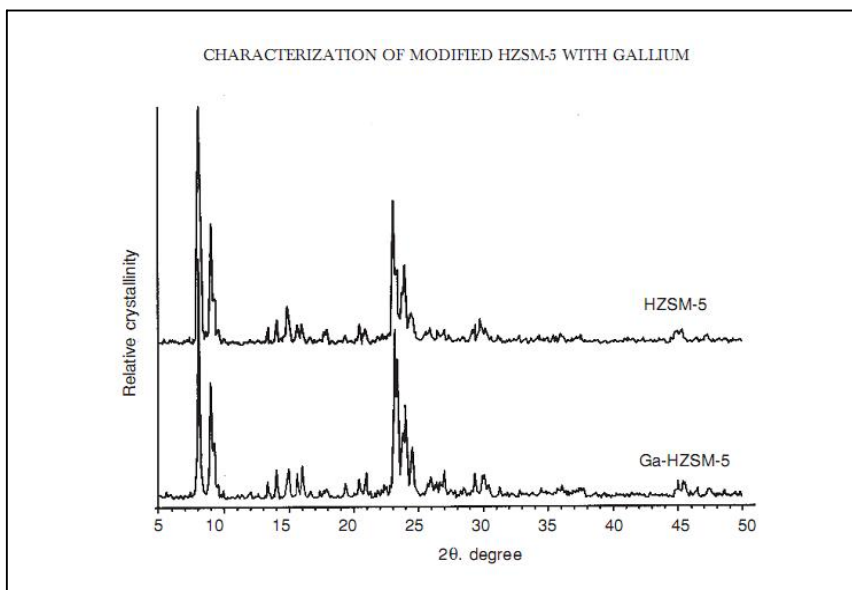


Figure 2.5 XRD diffractogram of HZSM-5 and Ga-HZSM-5 zeolite catalyst (Amin *et al.*, 2001)

Table 2.1 The Si/Al ratio and unit cell parameters of zeolites (Amin *et al.*, 2001)

Sample	The Si/Al ratio (*)			
	a (Å)	b(Å)	c(Å)	V(Å ³)
HZSM-5	19.674	20.725	14.665	5979.56
Ga-HZSM-5	19.505	20.627	13.825	5562.21

2.10 Characterization of Catalyst Using TPD

The acidity of the catalysts was examined by using temperature programmed desorption of ammonia. The amount of acid or acidity on a solid is expressed as moles of acid sites per unit weight of the solid. The amount of chemisorbed NH₃ on the HZSM-5 zeolite catalyst is much higher than Ga-HZSM-5. It indicates that the parent zeolite has more acid sites than the gallium zeolite. However, both low temperature (LT) and high temperature (HT) of Ga-HZSM-5 are lower than that of HZSM-5. Koval *et al.* (1996) reported that the desorption of NH₃ at the LT and HT is related to the acid strength of the zeolites. The result of the TPD is show in Table 2.2.

Both the zeolite catalyst contain LT and HT that suggest there is no significant changes in the acid strength, but Ga-HZSM-5 zeolite contains less number of acid sites than HZSM-5 zeolite. Topsøe *et al.* (1981) have postulated that the number of acid sites decreases as aluminium is removed from the crystal lattice and increases as aluminium is inserted into the framework of HZSM-5. The acidity also decreased with a decreasing micropore volume of HZSM-5, which caused a reduction in ammonia adsorption (Koval *et al.*, 1996). Based on the XRD, Si MAS NMR, and nitrogen adsorption data, the decrease in acidity is due to the effects of the removal of aluminium from the framework and metal oxide trapped inside the channels of modified zeolite.

Table 2.2 Nitrogen adsorption data (Amin *et al.*, 2001)

Sample	Amount of chemisorbed (moles/kg)	Low temperature (°C)	High temperature (°C)
HZSM-5	0.5424	214	415
Ga-HZSM-5	0.1418	209	414

2.11 Characterization of Catalyst Using TGA

TGA can be used to accurately detect the desorption of basic molecules from a zeolite as a function of temperature and the resulting data can be used to calculate the acid site strength and distribution of various zeolites (Bhatia *et.al.*, 1990).

2.12 Characterization of Catalyst Using FTIR

The infrared spectra for ZSM-5 and metal-loaded ZSM-5 samples are shown in figure 2.6. The structure sensitive absorption around 1200 and 550 cm^{-1} is of special interest to distinguish the zeolite types (Jansen *et al.*, 1984). In Table 2.2 the positions of some characteristic vibration bands are summarized. All samples have vibration bands between 546 and 1223 cm^{-1} . The frequency band at 1099 cm^{-1} is assigned to the asymmetric stretching of framework Si–O–Si or Si–O–Al bonds (Le Van Mao R *et al.*, 1999). The bands of Cr-ZSM-5 and Ga-ZSM-5 demonstrated a significant change in the frequency shift or a reduction in the intensity framework. This indicates that Cr-ZSM-5 and Ga-ZSM-5 catalysts experienced a significant change in the number of those forming framework bonds.

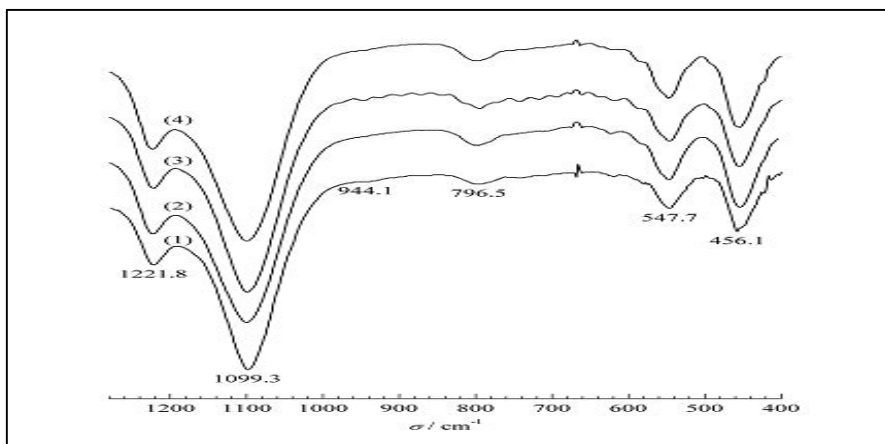


Figure 2.6 Infrared spectra (Amin *et al.*, 2003) (1) ZSM-5, (2) Cr-ZSM-5, (3) Cu-ZSM-5, (4) Ga-ZSM-5

Table 2.3 Infrared band positions of ZSM-5 and metal loaded ZSM-5 (Amin *et al.*, 2003)

Sample	Wavenumber (cm ⁻¹)				
	Asymmetric stretch		Symmetric stretch	Double ring	To bending
	External	Internal	External		
ZSM-5	1221.8	1099.3	796.5	547.7	456.1
Cr-ZSM-5	1223.7	1101.3	798.5	546.8	455.2
Cu-ZSM-5	1222.8	1100.3	795.6	545.8	457.1
Ga-ZSM-5	1223.7	1100.3	798.5	545.8	458.1

CHAPTER 3

METHODOLOGY

3.1 List of Materials

The Table 3.1 shows the list of materials that were used during the experiment of the studies.

Table 3.1 List of materials

No.	Materials	Purpose	Supplier
1	Zeolite A	Synthesis catalyst	Sigma-Aldrich Chemie
2	Iron sulfate		
3	Zinc sulfate		

3.2 Overall Methodology

Figure 3.1 shows the experimental work flow

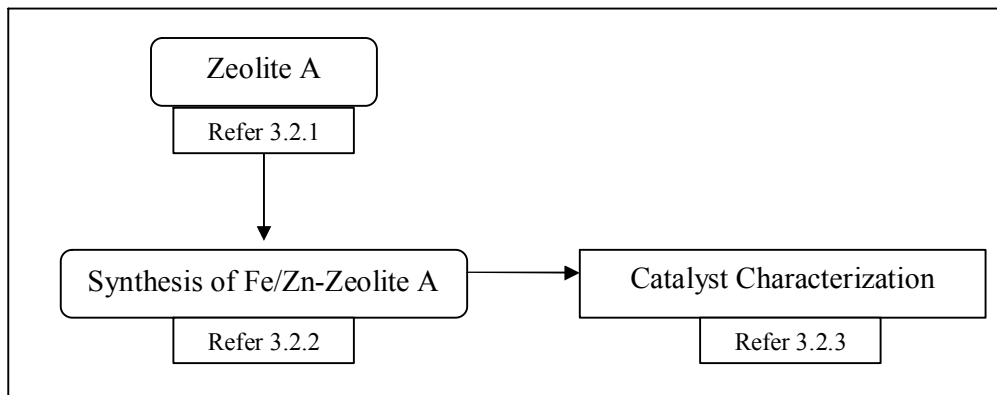


Figure 3.1 Experimental Work Flow

3.2.1 Zeolite A

Zeolite A was supplied by Sigma-Aldrich Chemie. The surface area of the zeolite is less than 45 micrometer.

3.2.2 Synthesis of Fe/Zn-Zeolite A

Iron nitrate, zinc nitrate, Zeolite-A and some water were mixed together with different mass ratio, this method called ion exchange method (Amin *et al.*, 2003). Table 3.2 shows the detail of the mass for each sample. Then the sample was dried at 100°C overnight and calcined at 550°C for 3 hours in an air flow.

Table 3.2 Mass of zinc, iron and zeolite for each sample

Component	Sample 1	Sample 2	Sample 3	Sample 4	Sample 5
Iron	0	0.2 gram	0.5 gram	0.8 gram	1 gram
Zinc	1 gram	0.8 gram	0.5 gram	0.2 gram	0
Zeolite	10 gram	10 gram	10 gram	10 gram	10 gram
Water	10 ml	10 ml	10 ml	10 ml	10 ml

3.2.3 Catalyst Characterization

The acid site, acid strength, thermal stability, structural and other physicochemical of the modified were measured using X-ray diffraction (XRD), Fourier transform infrared spectroscopy (FTIR) and thermo gravimetric analysis (TGA).

3.2.3.1 X-Ray Diffraction (XRD)

The XRD analysis was used to check the structure of the catalyst and presence of the crystalline phase. The XRD analysis was carried out at the Ibnu Sina Laboratory, Universiti Teknologi Malaysia. XRD measurements were performed in the range of $2\theta = 5^\circ$ to 50° using a siemen 5000 diffractometer with vertical goniometer and $\text{CuK}\alpha$ radiation ($\lambda = 1.542\text{\AA}$) at 35 kV and 35 mA (scanning speed: $4^\circ/\text{minute}$).

3.2.3.2 Fourier Transform Infrared Spectroscopy (FTIR)

FT-IR spectra were recorded on a Perkin Elmer Series II IR spectrometer at room temperature using KBr pellet technique. The sample was ground with the spectra grade KBr to form a pellet under hydraulic pressure. The pellet was used to

record the IR spectrum in the range of 400-1200 cm^{-1} under the atmospheric conditions with a resolution of 1 cm^{-1} .

3.2.3.3 Thermo Gravimetric Analysis (TGA)

The thermal stability of the catalysts was determined using a thermogravimetric analyzer (Perkin-Elmer TGA 7). The samples were placed in a pan that was heated under flow of air (25 ml/min) from room temperature to 1000°C at the heating rate of 10°C min^{-1} .

CHAPTER 4

RESULTS & DISCUSSION

4.1 XRD Characterization

Most of the structural information about Zeolite-A was obtained from X-ray diffraction (XRD). X-ray diffraction provides information about the average diameter of unit cell and the crystallinity of the zeolites, as shown in Table 4.1 based on the XRD diffractograms (Figure 4.1, Figure 4.2, Figure 4.3, Figure 4.4 and Figure 4.5). The diffractograms revealed that there is no change in the Zeolite-A crystalline structure after loaded with iron. The crystalline structure changes after zinc loaded on Zeolite-A as shown by the peaks at 2θ values of 16 and 24 appeared in sample 1, sample 2, sample 3 and sample 4.

Table 4.1 Crystallinity, average diameter of unit cell and rank average diameter of unit cell

Samples	Crystallinity (%)	Average diameter of unit cell (Å)	Rank average diameter of unit cell
Sample 1	23.2	3.67204	5
Sample 2	24.8	3.67621	3
Sample 3	38.3	3.67576	4
Sample 4	41.6	3.68064	2
Sample 5	53.5	3.6878	1

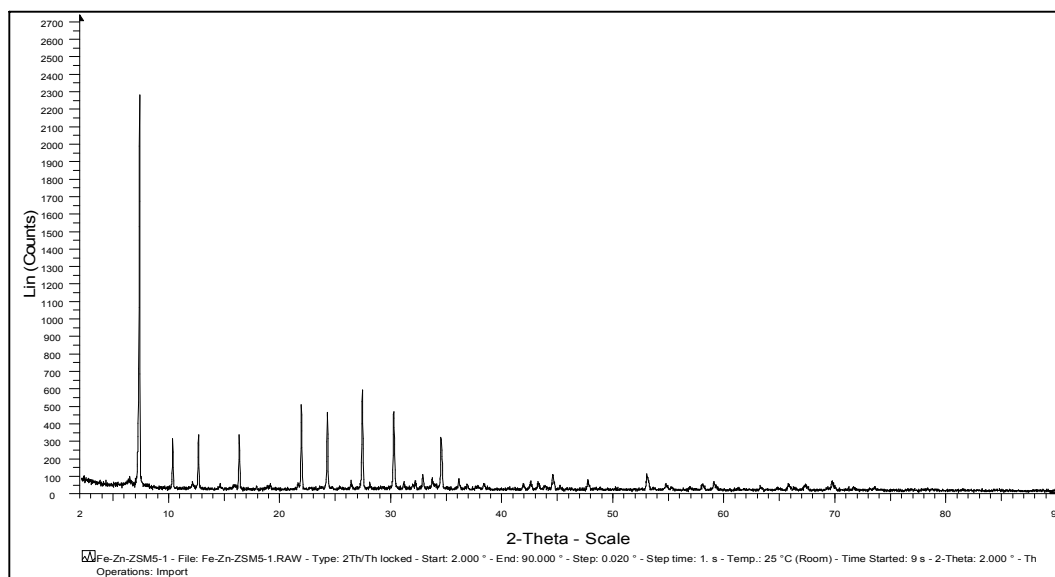


Figure 4.1 X-ray diffractogram of sample 1

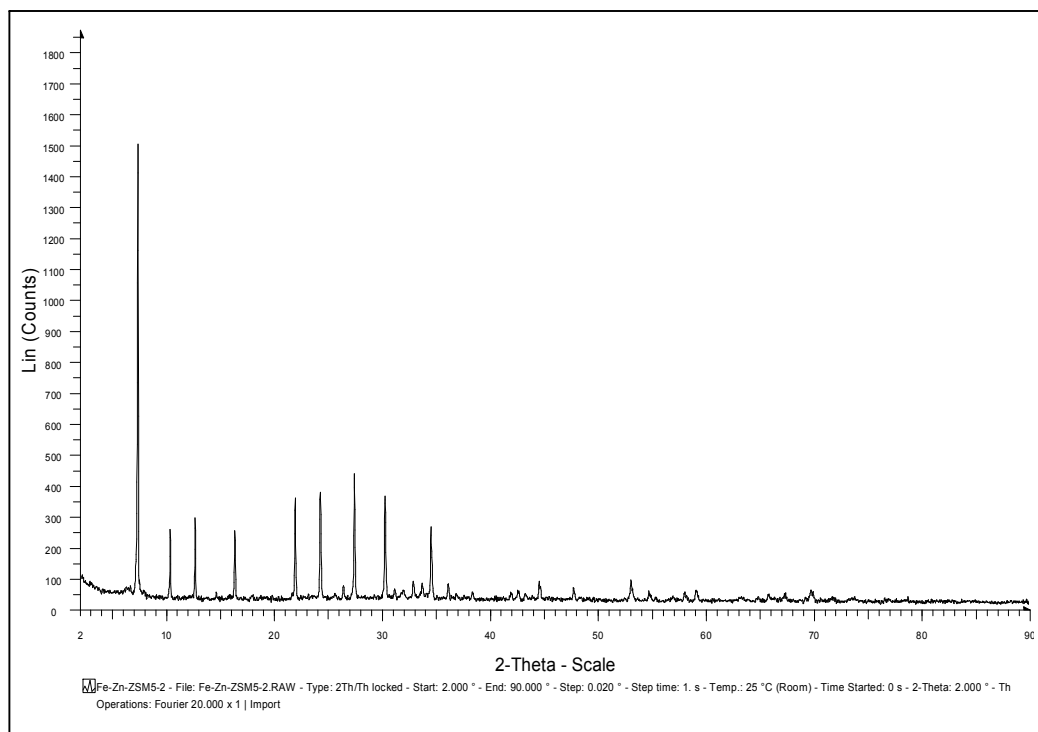


Figure 4.2 X-ray diffractogram of sample 2

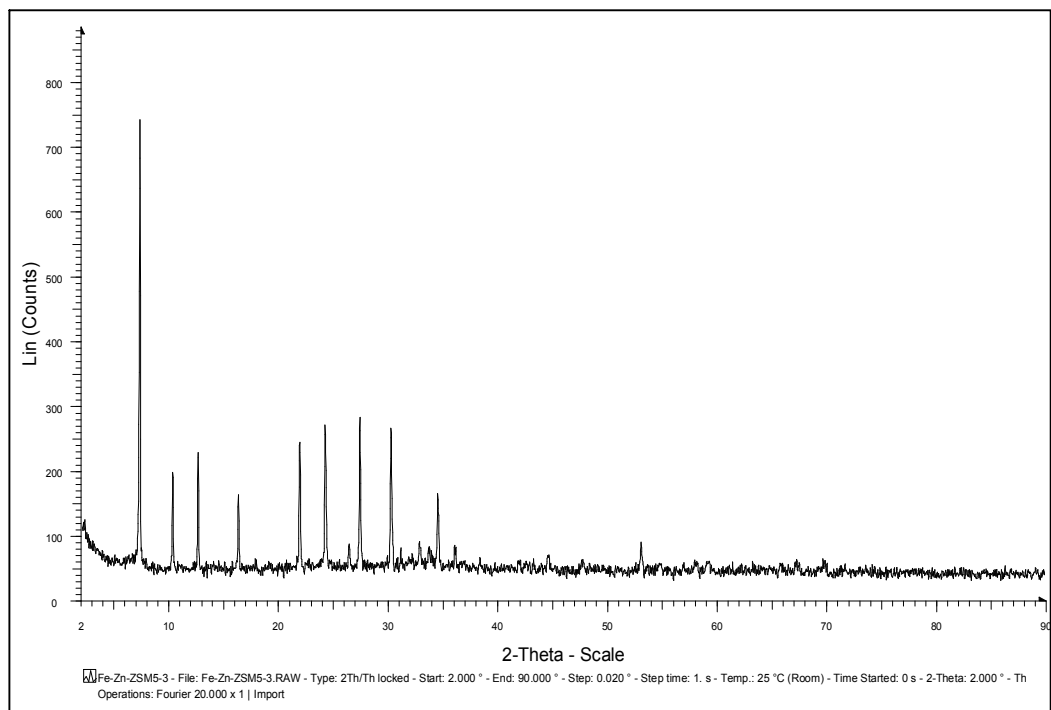


Figure 4.3 X-ray diffractogram of sample 3

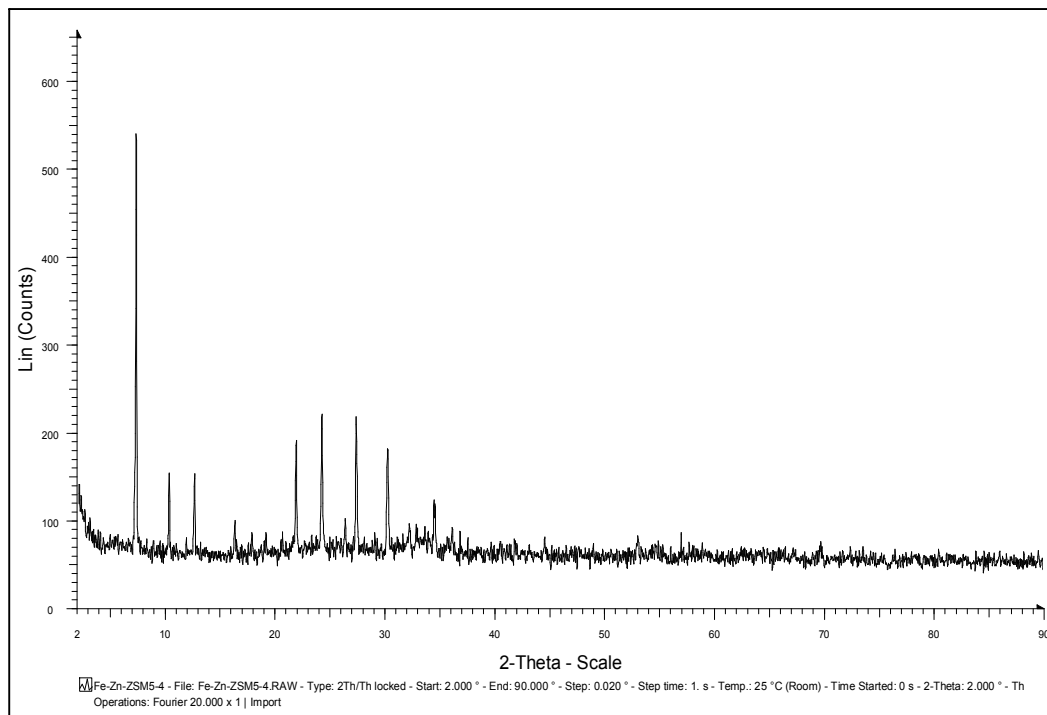


Figure 4.4 X-ray diffractogram of sample 4

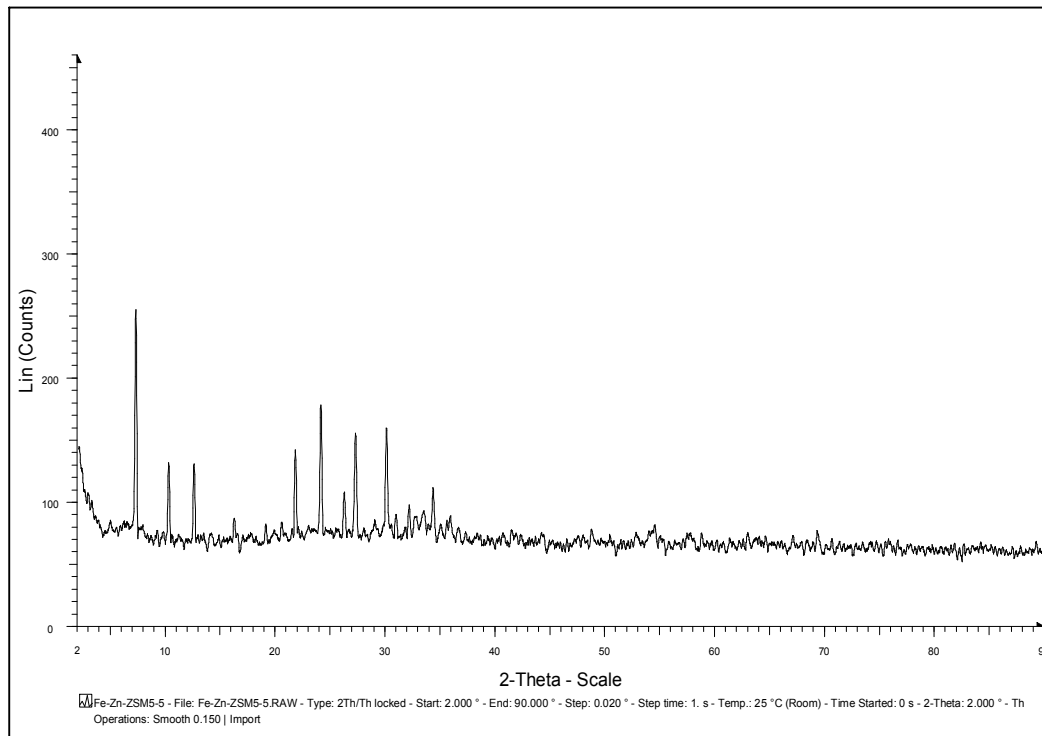


Figure 4.5 X-ray diffractogram of sample 5

The crystallinity of the zeolite can be calculated from the diffractograms. The crystallinity of the zeolite is expressed as the percentage of crystallinity using the intensity of the main peak at $2\theta=22.5-24.4$ in the XRD pattern (Amin *et. al.*, 2003). The crystallinities of Sample 1, Sample 2, Sample 3, Sample 4 and Sample 5 are 23.2, 24.8, 38.3, 41.6 and 53.5, respectively.

The results indicate that the crystallinity of the iron loaded Zeolite-A has increased the crystallinity. The change in crystalline structures were observed in the zinc and iron metal-loaded into Zeolite-A. The average diameter of unit cell of sample 1, sample 2, sample 3, sample 4 and sample 5 are 3.67204\AA , 3.67621\AA , 3.67576\AA , 3.68064\AA and 3.6878\AA , respectively and have been summarized in Table 4.1.

From the result, it shows that sample 5 has highest volume of unit cell and followed by sample 4, sample 2, sample 3 and sample 1. The removal of some of the aluminium from the zeolite framework could affect the average of unit cell (Amin *et.*

al., 2001). Iron content has increased the diameter of the Zeolite-A by replacing some of the aluminium from the zeolite framework.

Figure 4.1, Figure 4.2, Figure 4.3, Figure 4.4 and Figure 4.5 show the intensity of the diffractograms for each samples decrease from sample 1 until sample 5. The peak at $2\theta = 6.5-7.5$ for sample 1, sample 2, sample 3, sample 4 and sample 5 are 1990, 1560, 738, 548 and 383, respectively and have been summarize in Table 4.2.

Reported that the band intensities could be influenced by various factors such as the size of particles, the surface effect, and the dispersity of the metal, which resulted in a little change of the band intensity (Jia *et al.*, 1993). There is a gradual decrease in surface area with increasing iron content. The drop in surface areas may be attributed to micropore blockage by highly dispersed iron oxide particles (Debasish Das *et al.*, 1993).

Table 4.2 Intensity of the highest peak in x-ray diffractogram

Sample	Intensity of the highest peak
Sample 1	1990
Sample 2	1560
Sample 3	738
Sample 4	548
Sample 5	383

4.2 FTIR Characterization

Figure 4.6 shows the infrared spectra for sample 1, sample 2, sample 3, sample 4 and sample 5. The structure sensitive absorption around 1200 and 550 cm^{-1} is of special interest to distinguish the zeolite types (Jansen *et al.*, 1984). All samples have vibration band between 600 and 2400 cm^{-1} . The frequency band a 1099 cm^{-1} is

assigned to the asymmetric stretching of framework Si–O–Si or Si–O–Al bonds (Le Van Mao R *et al*, 1999).

The bands of sample 1, sample 2, sample 3 and sample 4 demonstrated significant changes in the frequency shift or a reduction in the intensity framework. This indicates that zinc content in the catalysts experienced a significant change in the number of those forming framework bonds. Except sample 5, there has a new intensity appear around $900 - 910 \text{ cm}^{-1}$.

In sample 4, wavenumber 1100cm^{-1} shows the catalyst form a new framework with the present of 8 percent of iron and 2 percent of zinc. Combination Zeolite-A with ratio 4:1 of iron and zinc affects the framework of catalyst. Beside that, sample 3 with ratio 1:1 of iron and zinc increases the intensity of the framework at wavenumber 729 and 692cm^{-1} .

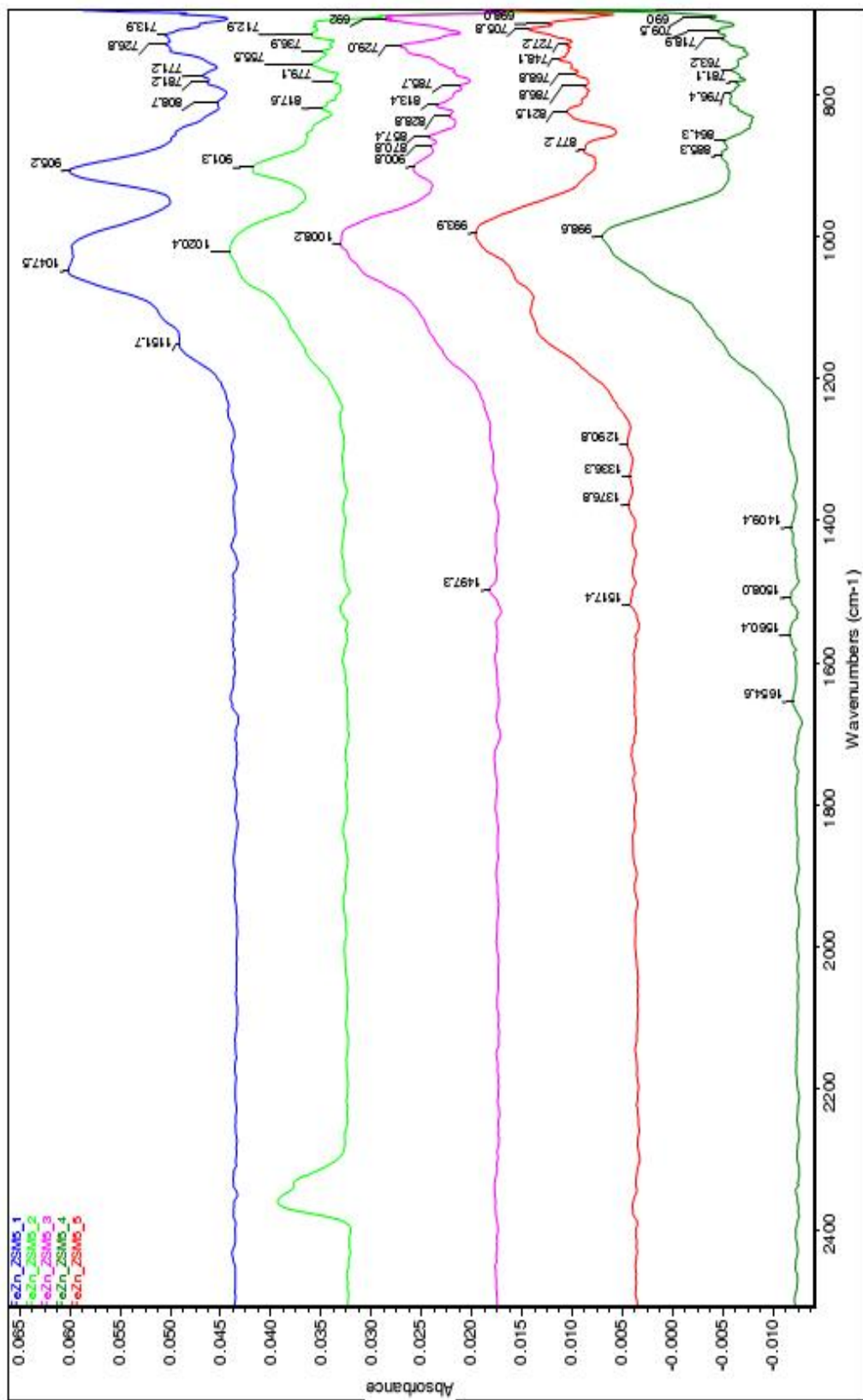


Figure 4.6 Wavenumber vs absorbance using FTIR

4.3 TGA Characterization

Thermo Gravimetric Analysis (TGA) characterization was done by using thermogravimetric analyzer (Perkin-Elmer TGA 7). TGA analysis was done for each sample in order to identify the thermal stability of the modified Zeolite-A. Figure 4.7 for sample 1, Figure 4.8 for sample 2, Figure 4.9 for sample 3, Figure 4.10 for sample 4 and Figure 4.11 for sample 5.

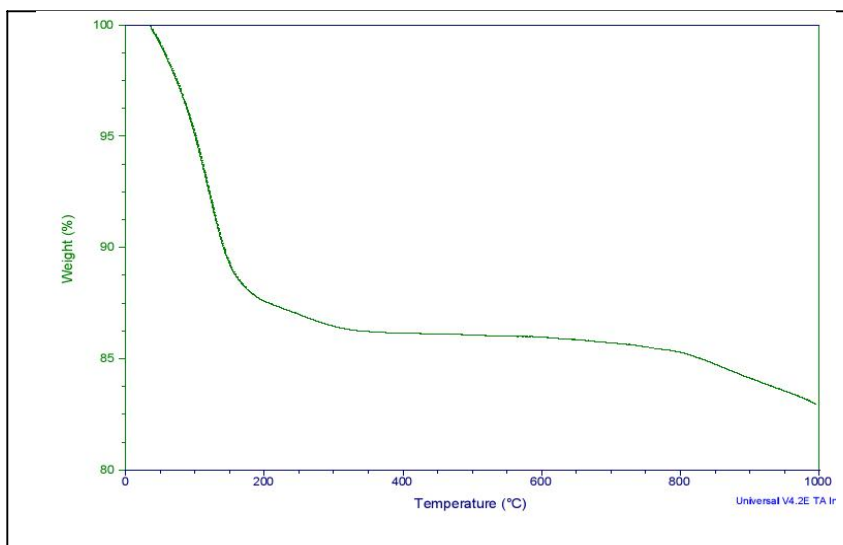


Figure 4.7 Weight Loss (%) vs Temperature for sample 1

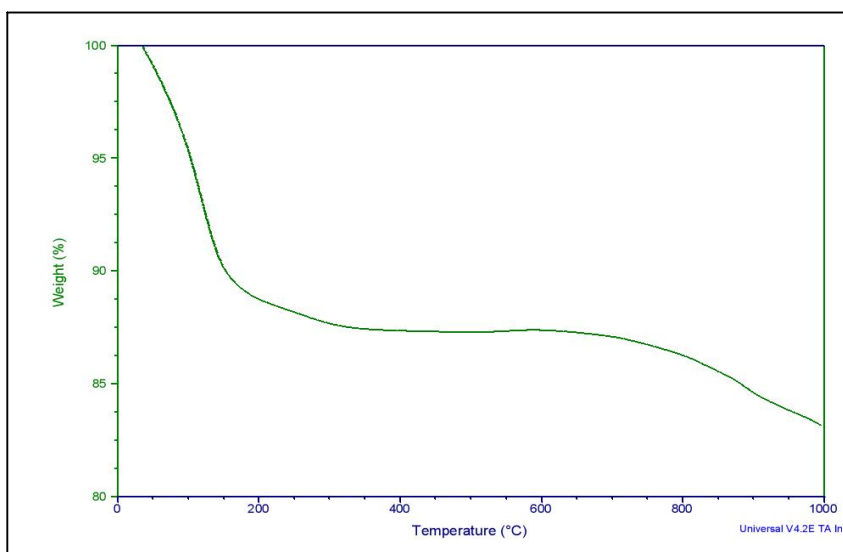


Figure 4.8 Weight Loss (%) vs Temperature for sample 2

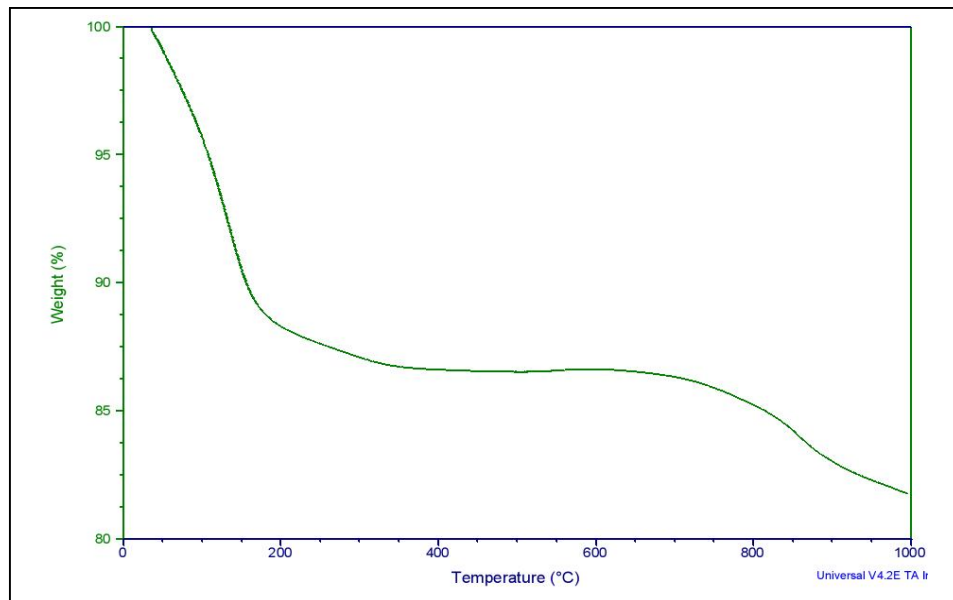


Figure 4.9 Weight Loss (%) vs Temperature for sample 3

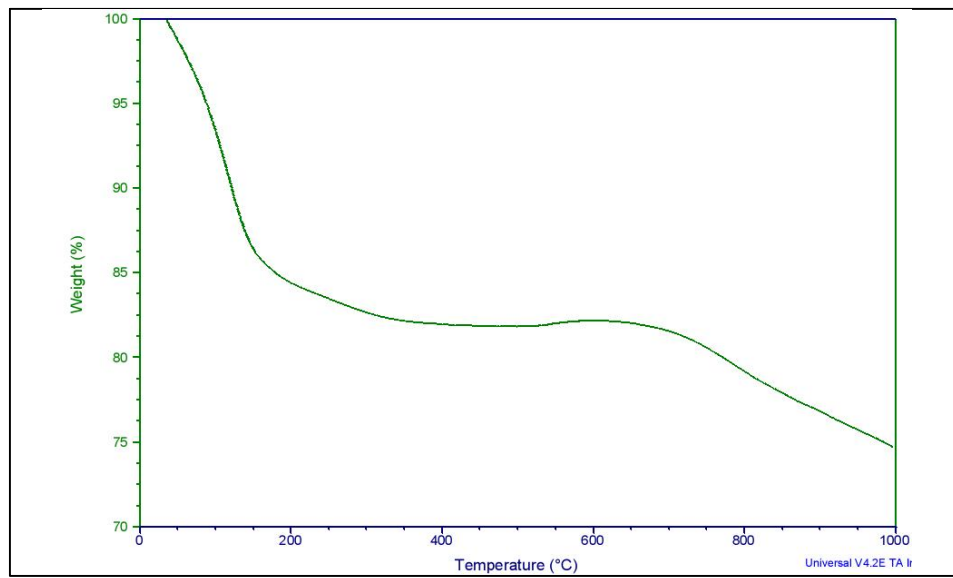


Figure 4.10 : Weight Loss (%) vs Temperature for sample 4

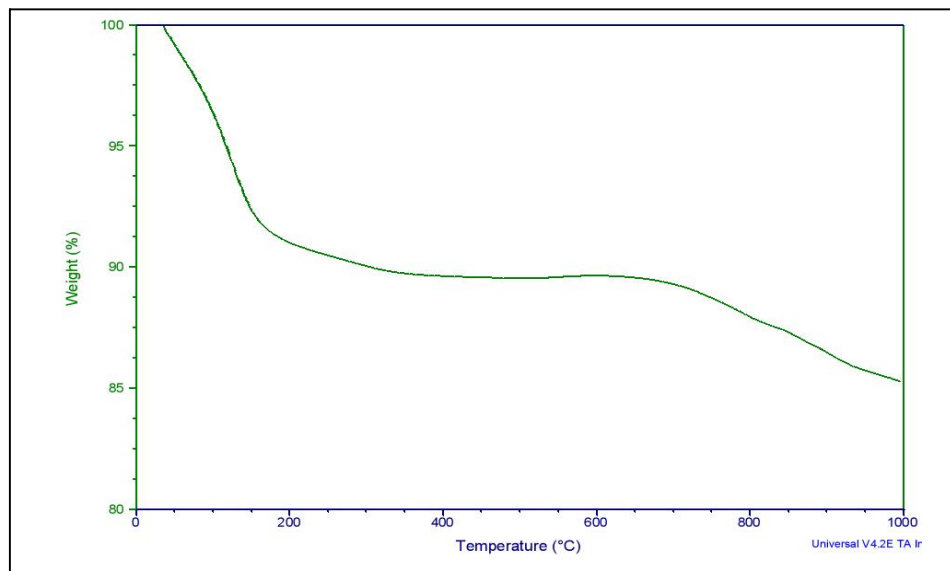


Figure 4.11 : Weight Loss (%) vs Temperature for sample 5

These figures are plotted by of weight loss versus temperature. The catalyst was heating from room temperature until 1000°C with the heating rate of 10°C per minute. Figure 4.7 was prepared with 10% of zinc content loaded into the catalyst. There are four situations occur on the catalyst during the heating. A weight loss of 11% has occurred in a short time starting from room temperature until 150°C. At this stage, all the moisture that attached on the catalyst has been removed.

The second stage occurs around 150°C until 350°C, the catalyst only has a small weight loss and the catalyst is stable with the increasing of the temperature. At the third stage from 350°C until 800°C, the weight loss of the catalyst seems does not occur. This stage is good to perform the methane conversion to liquid hydrocarbons. This is in line with the performance studies done by Amin *et. al.*, (2003). The final stage starts from 800°C until the highest temperature at 1000°C, at this stage the catalyst starts to decompose.

Result of TGA study for sample 2 is shown in Figure 4.8. The existent of zinc content at 2% of catalyst does not affect the thermal stability but affect the weight loss of the catalyst. Sample 2 has decreased the percentage of the weight loss of the catalyst as compared to the sample 1. The total weight loss for the sample 2 and

sample 1 at third stage are 12.5% and 13.75%, respectively. Since all the samples were prepared at the same condition, the content of all the catalyst's moisture were the same. The iron content in the sample 2 has supported the catalyst to decrease the total weight.

Figure 4.9 shows the result of sample 3. In this sample, the content of zinc and iron are 5% of the weight of catalyst. Combination of zinc and iron at same ratio has decreased the thermal stability of catalyst. The third stage of this sample starts at 350°C and end earlier as compared to sample 1 and 2 at 750°C. The increasing of iron content and decreasing of zinc content has affected the thermal stability. The total weight loss of sample 3 remains unchanged as compared to the sample 2 at 12.5%.

Sample 4 (Figure 4.10) has the highest weight loss of 17.5% until third stage, beside. The third stage of this sample occurs at 400°C until 650°C. The catalyst has started the third stage at higher temperature and ended at lower temperature. This sample was prepared with 2% of zinc content and 8% of iron content. This ratio of zinc and iron decreases the thermal stability and increases the percentage of weight loss. It can be concluded that the iron content should not higher than the zinc content in the same catalyst.

Sample 5 was prepared with 10% of iron content into Zeolite-A without zinc content. With existent of 10% of iron content without zinc content, this catalyst produces the lowest weight loss. The thermal stability of this sample is higher than the sampel 4 but it is lower than sampel 1 and sample 2. As compared to sample 3, sample 5 is better because sample 3 and sample 5 have same thermal stability but different weight loss. Result for sample 5 is shown in Figure 4.11.

4.4 General discussion

Table 4.3, Table 4.4 and Table 4.5 show the summary of the result of XRD, FTIR and TGA. Sample 1 shows the lowest percentage of crystallinity with the lowest average diameter of the unit cell but produces the highest surface area. It shows that the zinc content does not support the volume of the unit cell but increase the micropore volume and it also has low weight loss of the catalyst.

Table 4.3 Crystallinity, average diameter of unit cell and Intensity of the highest peak in x-ray diffractogram

Samples	Crystallinity (%)	Average diameter of unit cell (Å)	Intensity of the highest peak
Sample 1	23.2	3.67204	1990
Sample 2	24.8	3.67621	1560
Sample 3	38.3	3.67576	738
Sample 4	41.6	3.68064	548
Sample 5	53.5	3.6878	383

Table 4.4 Peak at $900 - 910 \text{ cm}^{-1}$ and changing of the samples in FTIR characterization

Samples	Peak at $900 - 910 \text{ cm}^{-1}$	Changing
Sample 1	yes	-
Sample 2	yes	-
Sample 3	yes	Increase intensity at 729 and 692 cm^{-1}
Sample 4	yes	New peak at 1100 cm^{-1}
Sample 5	no	-

Table 4.5 Result of TGA characterization

	First stage	Second stage	Third stage	Weight Loss
Sample 1	Room temperature until 150°C.	150°C to 350°C	350°C to 800°C	13.75%
Sample 2			350°C to 750°C	12.5%
Sample 3		150°C to 400°C		400°C to 750°C
Sample 4		150°C to 350°C	350°C to 750°C	10%
Sample 5				

Sample 2 has higher percentage of crystallinity, average diameter of unit cell and weight loss of the catalyst with existent of two percent of iron content in the catalyst but surface area of the catalyst is decreased. Sample 3 has increased the intensity of wavenumber at 729 and 692 cm^{-1} and this results a decrease in the size of the unit cell and the thermal stability of the catalyst.

Sample 4 has higher percentage of crystallinity and average diameter of unit cell but lower surface area and thermal stability. It also has highest weight loss of the catalyst. Sample 4 also produces a new peak at wavenumber 1100 cm^{-1} as compared to the other samples.

Sample 5 with 10% of iron content has the highest percentage of crystallinity and average diameter of the unit cell but lowest surface area. It also has lowest percentage of weight loss.

The absence of the iron content in the catalyst does not affect the framework and the crystalline of the catalyst but only affect the size of the unit cell and the surface area of the catalyst. As compare to zinc, it has modified the crystalline and framework of the catalyst. The results of the XRD, TGA and FTIR have shown effects these two metals in Zeolite-A.

Sample 2 with 8% of zinc and 2% of iron on Zeolite-A produces the most suitable catalyst for the methane conversion to liquid hydrocarbons. This sample has

high thermal stability, high surface area, and high average diameter of unit cell and has low weight loss. The higher performance of the methane conversion to liquid hydrocarbons is based on the surface area and the metal oxide that doped into the catalyst (Amin *et al*, 2003).

Zeolite doped with zinc is better than the parent zeolite and this indicates the increase of the concentration of olefins—precursors of aromatics in the reaction mixture due to the dehydrogenation activity of Zn species (Agáta Smiešková *et al.*, 2004). Iron content also increases the performance of methane to liquid hydrocarbons (Ammasi, S. *et al*, 2005).

CHAPTER 5

CONCLUSION & RECOMMENDATION

5.1 Conclusion

Results of this experiment show that zinc content improves the surface area of the catalyst and the iron content improve the thermal stability. Both of this metal needed in order to have higher conversion and selectivity of methane conversion. The iron content should not more than the zinc content because it will decrease the thermal stability

Iron content increases the thermal stability but decreases the surface area of the catalyst. However, zinc content increases the surface area. Sample 2 shows the suitable and perfect combination of zinc content and iron content because has high thermal stability, surface area and also has low percentage of weight loss.

5.2 Recommendation

The characterization study should including the characterization using NH₃-TPD. NH₃-TPD is used to identify the acid site of the catalyst such as bronsted and lewis acid site. The main physicochemical of catalyst for higher methane conversion is mainly base on the acid site (Amin *et al*, 2003). The higher acid site catalyst will produce the higher conversion of products. After the characterization, performance study should be continued in order to prove the result of the characterization.

REFERENCES

- Amin, N.A.S and Anggoro, D.A. (2002). Dealuminated ZSM-5 Zeolite Catalyst for Ethylene Oligomerization to Liquid Fuels. *Journal of Natural Gas Chemistry*.11: 79-86.
- Amin, N.A.S. and Anggoro, D.D. (2003). Characterization and Activity of Cr, Cu and Ga Modified ZSM-5 for Direct Conversion of Methane to Liquid Hydrocarbons.*Journal of Natural Gas Chemistry*. 12 : 123-134.
- Amin, N.A.S. and Kusmiyati. (2004). Improved Performance of W/HZSM-5 Catalysts for Dehydroaromatization of Methane, *Journal of Natural Gas Chemistry*. 13: 148-159.
- Aguiar, E. F. S, Appel, L.G. and Mota, C. (2005). Natural Gas Chemical Transformations: The Path to Refining in the Future. *Catalysis Today*. 101: 3-7.
- Anggoro, D.D 1998. Single Step Conversion of Methane to Gasoline: Effect of Metal Loaded HZSM-5 Zeolite Catalysts. Universiti Teknologi Malaysia. MSc Thesis
- Ammasi S., Dualbed Catalytic Reactor System for Direct Conversion Of Methane To Liquid Hydrocarbons, 2005.
- Bhatia, S., Beltramini, J., and Do, D.D., *Catalysis Today*, 7 (3), 309-435, (1990)

- Baerlocher, Ch. 2001. Zeolite Catalysis Principles and Applications
- Han, S., Martenak D. J., Palermo R. E. et al. J Catal, 1994, 148: 134
- Han, S., Kaufman E. A., Martenak D. J. et al. Catal Lett, 1994, 29: 27
- Hamid, S. A., Derouane E. G., Demortier G. et al. Appl Catal. A., 1994, 108: 85
- Jansen, J. C., Van Der Gaag, F. J., van Bekkum H. Zeolites, 1984, 4: 369
- Le Van Mao, R., Le. T. S., Fairbain, M. et. al. Appl. Catal. A., 1999, 185: 41
- O'Connor, C. T., Kojima M. Catal. Today, 1990, 6: 329
- Pak, S., Rades, T., Rosynek, M. P. et. al. Catal. Lett., 2000, 66: 1
- Pierella, L. B., Wang, L., Anunziata, O. A. React Kinet. Catal. Lett., 1997, 60: 101
- Mat, R. (1999), Reactivity Of Incorporated Copper In Boron-Zsm-5 Zeolite For Methane Conversion To Higher Hydrocarbons, Universiti Teknologi Malaysia.
- Mat, R. (2006), Modification of Zeolite HZSM-5 For Methane Conversion to Higher Hydrocarbon, Universiti Teknologi Malaysia.
- Mat, R., Amin, N.A.S and Abu Bakar, W.A.W. 1999. Preparation, Characterization and Catalytic Studies of Boron-HZSM-5 Zeolite for Methane Conversion to Higher Hydrocarbons. WEC Proceeding. K. Lumpur. 249–254

Ribeiro, F. R., et al., ed., Zeolites: Science and Technology, Martinus Nijhoff Publishers, The Hague, 1984.

Subhash Bhatia, Zeolite Catalysis: Principles and Applications, CRC Press, Inc., Boca Raton, Florida, 1990.

Thomas, S. and Dawe, R.A. (2003). Review of Ways to Transport Natural Gas Energy from Countries which Do Not Need the Gas For Domestic Use. *Energy*. 28: 1461-1477.

Vermeiren, W. J. M., I. D. M. L. Lenotte, J. A. Martens, and P. A. Jacobs. 1989. Zeolite-based Catalysts in the Oxidative Coupling of Methane into Higher Hydrocarbons. in Imarisio, G., Frias, M. and Bemtgen, J. M. Hydrocarbons Source of Energy. London: Graham & Trotman Ltd. 451– 460.

Vosloo, A.C. (2001). Fischer-Tropsch: a Futuristic View. *Fuel Processing Technology*. 71: 149-155.

Woolery, G L, Kuehl G H, Timken H C et al. *Zeolites*, 1997, 19: 288

Yagi, F., Kanai, R., Wakamatsu, S., Kajiyama, R., Suchiro, Y. and Shimura, M.(2005). Development of Synthesis Gas Production Catalyst and Process. *Catalysis Today*. 104: 2-6.

Zeng J L, Xiong Z T, Zhang H B et al. *Catal Lett*,1998, 53: 119, Xiong Zh T, Zhang H B, Lin G D et al. *Catal Lett*,2001, 74: 3

Zhang, A., Nakamura, I. and Fujimoto, K. (1997). A New Probe Reaction for Studying the Hydrogen Spillover Phenomenon. *Journal of Catalysis*. 168: 328-333.

Zhang, X., Gong, Y., Yu, G. and Xie, Y. (2002). Oxygen Species on NiO/Al₂O₃ and their Reactivities. *Journal of Molecular Catalysis A: Chemical*. 180: 293-298.

Zhang, X., Liu, J., Jing, Y. and Xie, Y. (2003). Support Effects on the Catalytic Behavior of NiO/Al₂O₃ for Oxidative Dehydrogenation of Ethane to Ethylene. *Applied Catalysis A: General*. 240: 143-150.

Zhu, J., Rahuman, M.S.M.M., Ommen, J.G.V. and L. Lefferts, L. (2004). Dual Catalyst Bed Concept for Catalytic Partial Oxidation of Methane to Synthesis Gas. *Applied Catalysis A: General*. 259: 95-100.

Zhu, J.Z., Ommen, J.G.V. and Lefferts, L. (2004). Reaction Scheme of Partial Oxidation of Methane to Synthesis Gas over Yttrium-stabilized Zirconia. *Journal of Catalysis*. 225: 388-397.

APPENDIX A

RESULT OF XRD CHARACTERIZATION

Table A1 : Result XRD Sample 1

Angle 2-Theta °	Average diameter Angstrom	Intensity Count	Intensity %
6.349	13.90912	72	3.6
7.221	12.23286	1990	100
10.263	8.61244	309	15.5
12.045	7.3421	64	3.2
12.581	7.03023	330	16.6
14.524	6.09388	53	2.7
15.845	5.58876	44	2.2
16.244	5.45238	331	16.6
19	4.66714	38	1.9
21.877	4.05946	505	25.4
24.218	3.67204	461	23.2
26.356	3.37885	71	3.6
27.367	3.25623	589	29.6
28.05	3.17847	60	3
30.204	2.95653	465	23.4
31.12	2.8716	65	3.3
32.103	2.78591	59	3
32.821	2.72659	103	5.2
33.712	2.65652	73	3.7
34.485	2.59871	317	15.9
36.08	2.4874	79	4
36.804	2.44009	47	2.4
38.364	2.34439	49	2.5
41.927	2.15305	48	2.4
42.579	2.12156	68	3.4
43.249	2.09023	64	3.2
43.885	2.0614	41	2.1
44.573	2.03118	102	5.1
45.243	2.00266	40	2
47.749	1.90323	67	3.4
53.081	1.72392	96	4.8
54.784	1.6743	54	2.7
58.091	1.58661	49	2.5

Table A2 : Result XRD Sample 2

Angle 2-Theta °	Average diameter Angstrom	Intensity Count	Intensity %
7.224	12.227	1560	100
10.218	8.65012	258	16.5
12.538	7.05434	312	20
14.518	6.09636	64	4.1
16.223	5.45933	274	17.6
17.851	4.96487	48	3.1
21.854	4.06363	369	23.7
24.19	3.67621	387	24.8
26.316	3.38389	86	5.5
27.347	3.25859	456	29.2
30.187	2.95823	404	25.9
31.097	2.87371	65	4.2
31.889	2.80406	68	4.4
32.822	2.7265	94	6
33.66	2.6605	80	5.1
34.461	2.60047	279	17.9
36.065	2.48843	80	5.1
38.312	2.34745	58	3.7
41.931	2.15283	59	3.8
42.542	2.12331	59	3.8
43.224	2.09139	58	3.7
44.549	2.03222	92	5.9
47.705	1.90489	71	4.6
53.038	1.72521	94	6
54.718	1.67617	60	3.8
55.335	1.65893	35	2.2
56.94	1.6159	44	2.8
58.022	1.58833	59	3.8
59.084	1.56229	69	4.4
65.817	1.41782	53	3.4
67.345	1.38932	40	2.6
69.757	1.34705	65	4.2

Table A3 : Result XRD Sample 3

Angle 2-Theta °	Average diameter Angstrom	Intensity Count	Intensity %
7.235	12.2079	738	100
10.25	8.6233	198	26.8
12.574	7.03404	241	32.7
13.983	6.32824	71	9.6
16.253	5.44933	165	22.4
17.84	4.96791	56	7.6
21.849	4.06456	247	33.5
24.193	3.67576	283	38.3
26.359	3.37844	90	12.2
27.35	3.25829	282	38.2
30.206	2.95642	268	36.3
31.098	2.87362	95	12.9
32.803	2.72799	93	12.6
33.663	2.66026	75	10.2
34.471	2.59976	180	24.4
36.105	2.48576	89	12.1
38.32	2.34699	73	9.9
43.2	2.0925	64	8.7
44.562	2.03165	79	10.7
46.39	1.95577	57	7.7
48.341	1.88129	66	8.9
51.893	1.76055	56	7.6
53.051	1.72482	93	12.6
53.654	1.70686	54	7.3
58.189	1.58415	60	8.1
59.265	1.55793	57	7.7
62.588	1.48298	53	7.2
65.816	1.41784	64	8.7
65.88	1.41662	63	8.5
67.494	1.38661	63	8.5
69.866	1.34523	67	9.1
71.322	1.3213	51	6.9
82.544	1.16777	52	7
82.775	1.16509	55	7.5
86.316	1.12615	54	7.3

Table A4 : Result XRD Sample 4

Angle 2-Theta °	Average diameter Angstrom	Intensity Count	Intensity %
7.241	12.19824	548	100
10.239	8.63235	160	29.2
12.557	7.04374	149	27.2
16.234	5.45557	112	20.4
17.83	4.97075	85	15.5
19.04	4.65742	87	15.9
20.555	4.31751	94	17.2
21.826	4.0688	184	33.6
24.161	3.68064	228	41.6
26.299	3.386	110	20.1
27.324	3.26126	220	40.1
30.177	2.95913	196	35.8
32.16	2.78107	97	17.7
32.821	2.72655	95	17.3
34.465	2.60017	110	20.1
36.065	2.48841	103	18.8
36.84	2.43781	78	14.2
52.999	1.72639	85	15.5

Table A5 : Result XRD Sample 5

Angle 2-Theta °	Average diameter Angstrom	Intensity Count	Intensity %
7.204	12.26022	383	100
10.202	8.66372	162	42.3
12.536	7.05533	183	47.8
16.215	5.462	93	24.3
19.074	4.64918	92	24
21.779	4.07754	173	45.2
24.113	3.6878	205	53.5
26.242	3.39329	109	28.5
27.274	3.26719	165	43.1
30.096	2.96693	203	53
30.963	2.88582	109	28.5
32.164	2.78077	97	25.3
34.353	2.60839	125	32.6
58.858	1.56775	84	21.9